



Single walled carbon nanotubes with encapsulated Pt(II) photocatalyst for the oxidation of sulfides in water

Daniel González-Muñoz^a, José Alemán^{a,b,c,*}, Matías Blanco^{a,*}, Silvia Cabrera^{b,d,*}

^a Organic Chemistry Department, Science Faculty, Universidad Autónoma de Madrid, 28049 Madrid, Spain

^b Institute for Advanced Research in Chemical Sciences (IAChem), Universidad Autónoma de Madrid, Madrid, Spain

^c Center for Innovation in Advanced Chemistry (ORFEO-CINQA), Universidad Autónoma de Madrid, Madrid 28049, Spain

^d Inorganic Chemistry Department, Science Faculty, Universidad Autónoma de Madrid, Madrid 28049, Spain

ARTICLE INFO

Article history:

Received 5 April 2022

Revised 26 May 2022

Accepted 16 June 2022

Available online 25 June 2022

Keywords:

Pt(II) complexes
Carbon nanotubes
Encapsulation
Photocatalysis
Water-reactions

ABSTRACT

A simple one-step synthesis of a heterogeneous photocatalyst based on the encapsulation of the quinolate-platinum complex **1** in the inner cavity of Single Walled Carbon Nanotubes (**Pt1@oSWNT**) is presented. This strategy generates a robust and stable catalyst for photooxidations performed in water media. **Pt1@oSWNT** is characterized spectroscopically and microscopically to have encapsulated a 2.5 % wt. of the unaltered complex. This material, which only contained 0.04 mol% of **1**, is able to chemoselectively yield a wide variety of sulfoxides in water in the presence of air under 385 nm irradiation. The catalyst also presents affinity for polyaromatic substrates, increasing the reaction rate as a function of the number of condensed rings, achieving turnover frequencies as high as 8187 h⁻¹. Moreover, the heterogeneous catalyst could be recycled for more than six consecutive reaction runs without losing its catalytic activity or detecting catalyst leaching.

© 2022 The Author(s). Published by Elsevier Inc. This is an open access article under the CC BY license (<http://creativecommons.org/licenses/by/4.0/>).

1. Introduction

The chemoselective oxidation of sulfides to sulfoxides is a relevant transformation for the preparation of pharmaceuticals, natural products, ligands, and key intermediates in organic synthesis [1]. Traditionally, such oxidation process has been carried out using peracids or peroxides as oxidants (*m*-CPBA, peracetic acid) or conducted through metal catalysis. However, under those conditions, the chemoselective oxidation to sulfoxides, without the appearance of sulfones as byproduct, is not fully achieved. Besides, from an industrial standpoint, the main drawbacks are the safety aspects of handling those hazards oxidants. Consequently, a more chemoselective and milder methodology for the oxidation of sulfides is required. In this context, the oxidation of sulfides using oxygen as oxidant, light as chemical vector and a photocatalyst has provided, during the last years, an environmentally friendly alternative to the above-mentioned traditional process [2,3]. Different heterogeneous photocatalysts based on covalent organic frameworks (COF) [4], metal organic frameworks (MOF) [5], polymers [6] or polyoxometalates [7] among others, have been studied

for the heterogeneous photooxidation of sulfides. Such heterogeneous catalysts were recyclable systems with variable catalytic activity, needing, in most cases, the use of saturated-O₂ solutions or pure O₂ atmosphere to reduce reaction times. On another hand, the best catalytic performance achieved using both homogeneous or heterogeneous photocatalytic systems requires the use of organic solvents such as acetonitrile, dichloromethane or methanol, and few of them are reported to be active in water [8]. The loss of activity of the photocatalysts in water is ascribed to the insolubility and self-assembly in the case of organic photocatalysts, or the instability of metal-based compounds and materials. Consequently, the development of water-compatible photocatalytic systems remains a major challenge.

Very recently, we developed a new family of photocatalytic platinum complexes that were successfully used for a large variety of different reactions such as the alkylation of aldehydes or the oxidation of boronic acids and sulfides [3b,d]. In most of the cases, we employed organic solvents such as DMF and DMSO, founding that the platinum complex was very difficult to be recovered and reused. In this sense, we studied its incorporation into mesoporous silica [9]. For this objective, the heterogeneous material requires several steps to be synthesized (see Fig. 1a). It was necessary to prepare the corresponding ligand, the platinum complex and then functionalize the mesoporous silica. The covalent attachment of

* Corresponding authors.

E-mail addresses: jose.aleman@uam.es (J. Alemán), matias.blanco@uam.es (M. Blanco), silvia.cabrera@uam.es (S. Cabrera).

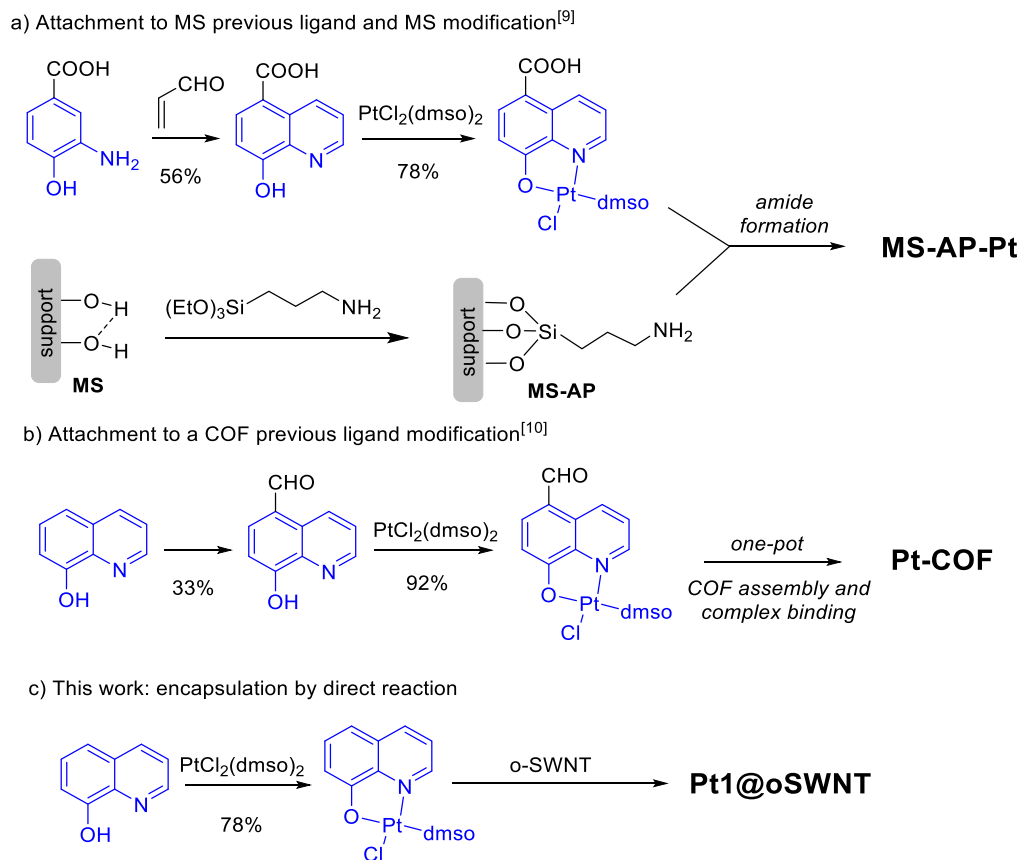


Fig. 1. Different strategies for anchoring photocatalysts into materials.

the complex to the material through amide coupling protocols allowed the synthesis of the desired photocatalytic material (MS-AP-Pt). Alternatively, the incorporation of the platinum structure into a COF material was also explored [10]. Again, the synthesis of a modified aldehyde-platinum complex for its incorporation into the laminar material was necessary (Pt-COF, Fig. 1b). Therefore, tedious synthesis and derivatization of these complexes were needed to prepare the different heterogeneous photocatalytic materials.

In the last decade, the use of single-walled carbon nanotubes (SWNT) to prepare heterogeneous photocatalysts have demonstrated to be an ideal approach to get enhanced catalytic performance due to the good electronic communication among the material and the photocatalyst [11]. The functionalization of SWNT with the photocatalyst has been mainly performed via two different strategies: a) physisorption of the catalyst at the nanotube surface [12] or b) covalent bond between both units [13]. In addition, we also reported a novel functionalization approach, the endohedral functionalization, that consist of the introduction of the photocatalyst, 10-phenylphenothiazine, in the inner cavity of the SWNT [14]. This approach does not require the modification of the photocatalyst to be linked to the material, and we demonstrated that the stability of the photocatalyst is preserved. Therefore, the endohedral functionalization of SWNT with the platinum photocatalyst will allow an easy use and recovery without the need of modification of the structure of the metal complex. Moreover, we also want to study its photocatalytic activity in the oxidation of sulfides in aqueous media for the development of more sustainable photocatalytic processes.

2. Experimental section

2.1. Materials and methods

All chemicals and reagents, including Single Walled Carbon Nanotubes employed in this work (1.4 nm in average diameter, μm in length, Merck), were purchased from commercial sources (reagent grade quality or higher) and used without further purification, whereas anhydrous solvents were taken from a Solvent Purification System (SPS) dispenser or purchased from commercial sources. Chromatographic purification of organic products was accomplished by flash chromatography using silica gel (Merck Geduran® Si 60). The synthesis of substrates **2k** and **2l**, including the corresponding spectroscopic characterization, is fully reported at the [supporting information](#).

NMR spectra were acquired on a BRUKER AVANCE spectrometer running at 300 MHz for ^1H (75 MHz for ^{13}C) and are internally referenced to residual solvent signals (CDCl_3 referenced at δ 7.26 ppm, $\text{DMSO-}d_6$ referenced at δ 2.50 ppm for ^1H NMR). Data for ^1H NMR are reported as follows: chemical shift (δ ppm), multiplicity (s = singlet, d = doublet, dd = doublet of doublets, t = triplet, m = multiplet), coupling constant J (Hz) and integration. Data for ^{13}C NMR are reported as chemical shift (δ ppm). Electrospray Ionization Mass Spectra (ESI-MS) were obtained on an Agilent Technologies 6120 Quadrupole LC/MS coupled with a Supercritical Fluid Chromatograph (SFC) Agilent Technologies 1260 Infinity Series instrument. The UV–visible absorption spectroscopy data were acquired using an Agilent 8453 UV–Vis Spectrophotometer controlled by UV–Visible ChemStation Software, in the 200–800 nm range. In this case, powder samples were dispersed in methanol

(HPLC grade), forming a stable colloidal dispersion, while complex **1** was measured as a homogeneous solution. Raman spectra were acquired with a Bruker Senterra confocal Raman microscope instrument equipped with 532, 633, and 785 nm excitation lasers. TEM images were obtained with JEOL-JEM 2100F instrument, equipped with an EDX Oxford microprobe. Samples were drop-casted from the aforementioned methanol suspensions on holey-carbon copper grids. TXRF analysis were carried out in a S2 Picofux (Bruker) with a current of 600 μ A and 50 kV. TXRF system was equipped with a Mo X-ray source working at 50 kV and 600 μ A, a multilayer monochromator with 80% of reflectivity at 17.5 keV (Mo K α), a XFlash SDD detector with an effective area of 30 mm² and an energy resolution better than 150 eV for 5.9 keV (Mn K γ). For deconvolution and integration, commercial Spectra v. 7.5.3 software package from Bruker was used. Emission spectra of the light source used for the photochemical reactions was recorded on an optical spectrometer StellarNet model Blue-Wave UV-NB50. The reactor consisted of a custom-made temperature-controlled system, where the reaction mixture was kept at room temperature by passing coolant through the metallic system employing a recirculating chiller, and the irradiation was achieved with a single LED (385 nm) located 1 cm beneath the base of the vial.

2.2. Synthesis of homogeneous complex **1**

0.47 mmol of 8-hydroxyquinoline was suspended in a solution of NaOH (0.56 mmol) in 0.3 mL of MeOH. The resulting suspension was stirred until the ligand was completely dissolved, where a suspension of *cis*-PtCl₂(dmsol)₂ (0.45 mmol) in 0.6 mL of acetone was added. The reaction was maintained for 24 h at room temperature and the solid product was then filtered, washed with cold water and ether, and dried under vacuum (scheme 1) to yield a yellow solid which was labelled as homogeneous complex **1**, and obtained in 78% yield. Spectroscopic data are in agreement with the published data [15].

¹H NMR (300 MHz, DMSO *d*₆): δ 9.38 (d, *J* = 4.6 Hz, 1H), 8.66 (d, *J* = 8.7 Hz, 1H), 7.70 (dd, *J* = 8.3, 4.9 Hz, 1H), 7.49 (t, *J* = 7.8 Hz, 1H), 7.17 (d, *J* = 7.9 Hz, 1H), 7.01 (d, *J* = 8.0 Hz, 1H), 3.61 (s, 6H).

2.3. Nanotubes opening

In a typical experiment [14], 50 mg of pristine and closed SWNT were suspended in 50 mL of concentrated hydrochloric acid, and the mixture was stirred at 60 °C for 2 h. After cooling down, the solid was isolated by centrifugation and washed with water with the necessary centrifugation cycles till the supernatant reached neutral pH. After drying under vacuum, the procedure yielded the sample **oSWNT**.

2.4. Encapsulation of complex **1**

In a typical experiment [14], 100 mg of complex **1** and 10 mg of **oSWNT** were suspended, under nitrogen atmosphere, in 4 mL of N₂-degassed dimethylsulfoxide (DMSO) and the mixture was magnetically stirred at 150 °C for 16 h. Then, the suspension was filtered through a 0.45 μ m polypropylene (PP) membrane. The black powder was collected, suspended in 20 mL of fresh DMSO with the help of 5 min of sonication, and filtered again. This washing procedure was repeated 5 additional times with DMSO and 5 additional cleaning cycles employing dichloromethane (DCM). Drying under vacuum yielded the sample **Pt1@oSWNT**.

2.5. Catalytic light-driven sulfide oxidation

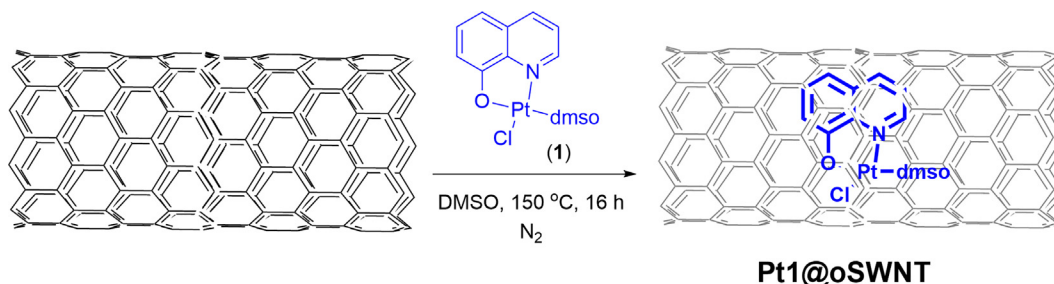
A vial was charged with a magnetic stirring bar, the organic substrate **2a-k** (0.1 mmol), the catalyst (1 mg for nanotubes-based materials, 0.04 mol% for complex **1**) and H₂O (1 mL). The vial was sealed and irradiated at 385 nm LED at room temperature for the desired time, typically 6 h. A 0.05–0.1 mL aliquot was withdrawn at regular intervals and analyzed by NMR spectroscopy to monitor the progress of the reaction. Yields, unless otherwise stated, were determined by isolation of the product through filtration from the reaction medium by adding the minimum amount possible of acetone and further vacuum-drying.

2.6. Catalyst recovery, leaching and mechanistic experiments

Once the reaction was completed, **Pt1@oSWNT** was recovered by filtration over a PP membrane and then washed with 3 cycles of acetone-H₂O, sonicating for 5 min between each cycle. Then, sample was vacuum-dried. After that, the heterogeneous catalyst was submitted to a new catalytic cycle by adding sulfide **2a** and 1 mL of water. This procedure was repeated several times. In the case of the homogeneous photocatalyst, endurance tests were performed by adding a fresh amount of **2a** (0.1 mmol) to the vial after reaction completion for several times.

For the leaching experiments, a typical hot-filtration configuration was adopted. To perform this task, the reaction with **2a** as substrate was allowed to proceed for a desired time under the standard conditions. Then, at 150 min of reaction (~50% conversion), the reaction was removed from the LED, the nanotube based catalyst was filtrated off, and the filtrate was submitted to irradiation. This filtrate was monitored by withdrawing aliquots at regular intervals and analyzed by NMR spectroscopy. The procedure was repeated as well with the oxidation of **2a** after 200 min (~90% conversion).

For the quenching experiments, the general reaction set-up was employed but adding 0.5 equivalents (0.05 mmol) of sodium azide or 1,4-dimethoxybenzene as scavengers. A 0.05 mL aliquot was withdrawn from the reaction after 6 h and analyzed by NMR.



Scheme 1. Encapsulation procedure to obtain the sample **Pt1@oSWNT**.

3. Results and discussion

First, the Pt-quinolinate complex **1** was synthesized following a procedure reported previously by us [15]. To perform the encapsulation of complex **1**, pristine SWNT were opened employing a mild acid treatment with HCl for 2 h, yielding the sample **oSWNT** (denoting opened-SWNT) [14]. High resolution transmission electron microscopy (HRTEM) confirmed that, in agreement with previous reports [16], all the semispherical carbon caps, the amorphous carbon and the metal nanoparticles responsible of the nanotubes growing were removed. Thus, **oSWNT** sample is observed as opened, clean and smooth nanotubes (see Fig. S2 at SI). Next, the encapsulation of complex **1** in **oSWNT** was conducted by heating at 150 °C **oSWNT** in the presence of **1** in dimethyl sulfoxide (DMSO) (Scheme 1). The resulting solid was washed with fresh DMSO, acetone and dichloromethane to yield **Pt1@oSWNT**.

The heterogeneous photocatalyst **Pt1@oSWNT** was fully characterized using different techniques. Firstly, the analysis of the sample by HRTEM determined that the structural integrity of the nanotubes was preserved after the hot treatment in DMSO (Fig. 2). Indeed, smooth tubes were observed after TEM exhaustive analysis without any deformation, rupture or shortening. In addition, the presence of adequate size objects lying sandwiched between the walls of the nanotube clearly came across within the observation areas (see arrows Fig. 2b). Those objects, whose diameter ranged 0.6–0.8 nm (considering the Brownian motion and the high magnification of the instrument that may cause decomposition due to beam damage) were not visualized in the precursor sample **oSWNT** (Fig. 2a). This observation seems to indicate that the Pt complex **1** was able to enter in the inner cavity of the nanotube. Even considering that those objects could be set above or underneath an individual random nanotube, the probabil-

ity that all the observed objects during the whole TEM analysis lied within that “outside” π -stuck physisorbed configuration is very low. Therefore, the imaging must correspond to the encapsulation of a molecule object in the inner cavity of the nanotubes. Besides, upon zooming up those regions, elongated structures containing bright spots that matches the size of complex **1** unit can be seen. Moreover, the EDX microprobe detected Pt units at the observation areas, further confirming that the detected objects must correspond to the complexes moieties (Fig. 2b, lower panels). Finally, no molecules could be clearly detected outside the nanotubes, excluding the possibility of non-encapsulated Pt complexes (**1**) in the sample. Encapsulated samples reported previously in the literature agreed with this morphological observation [14].

Next, Raman spectroscopy was carried out to compare the spectral features of the precursor **oSWNT** with the functionalized sample **Pt1@oSWNT** (Fig. 3). Analysing the spectrum of **oSWNT** sample, the Raman pattern agrees with the presence of high-purity SWNT. Hence, an intense G band at $\sim 1580\text{ cm}^{-1}$ (attributed to the tangential C-C sp^2 vibrational mode) is detected as the most prominent spectral feature. This band appears with a very small D band at $\sim 1340\text{ cm}^{-1}$ (related with the C- sp^3 vibrations). Indeed, the I_D/I_G ratio (standard structure quality parameter) for this pristine sample is calculated to be 0.04. In addition, a unique SWNT band related to the radial vibrations of the carbon atoms in the tubular conformation (the radial breathing mode, RBM) was observed at $\sim 200\text{ cm}^{-1}$, which agrees with the diameter of 1.3–1.4 nm observed by HRTEM. Regarding the spectrum of **Pt1@oSWNT**, all the typical Raman features are also observed, though slight differences can be detected. On one hand, the I_D/I_G ratio of the encapsulated sample is increased to 0.11 as a result of the hot treatment in DMSO (a control sample with bare nanotubes refluxed in DMSO for 16 h afforded the same result, see

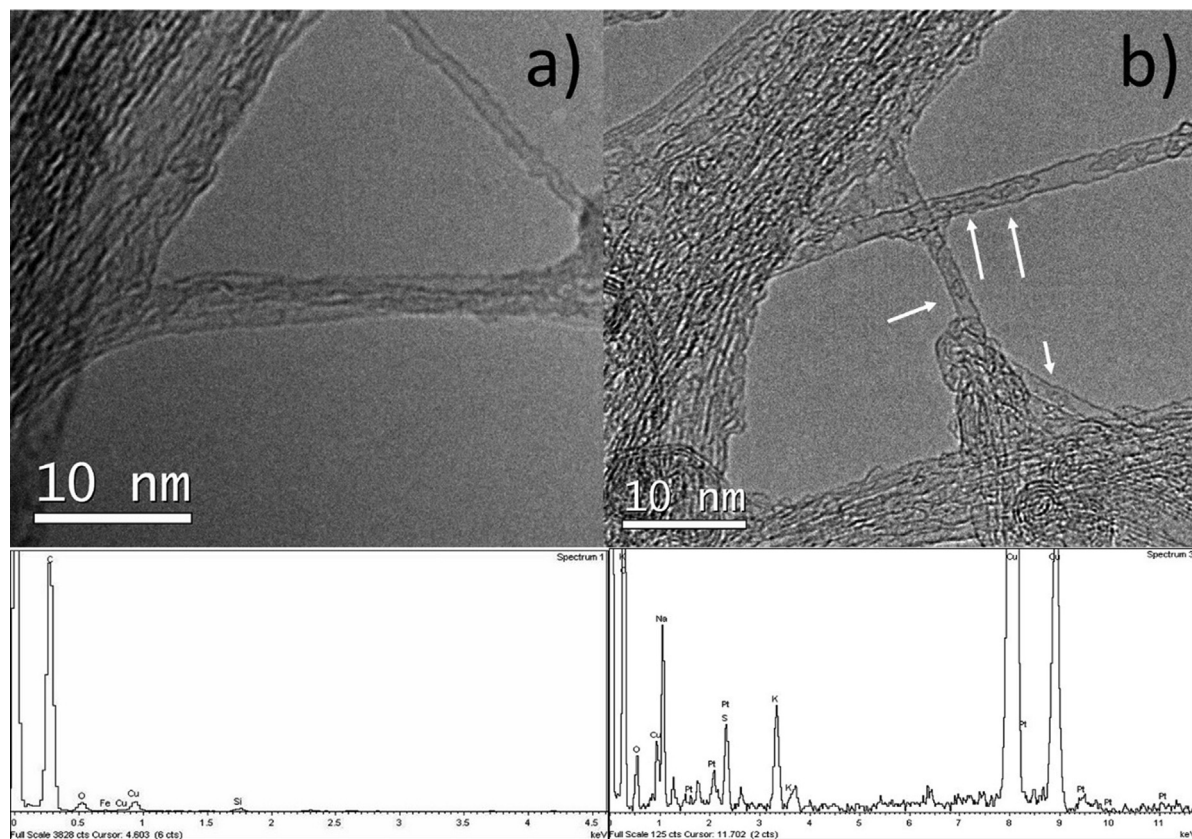


Fig. 2. HRTEM of a) **oSWNT**, b) **Pt1@oSWNT** Lower panels: the corresponding EDX spectra.

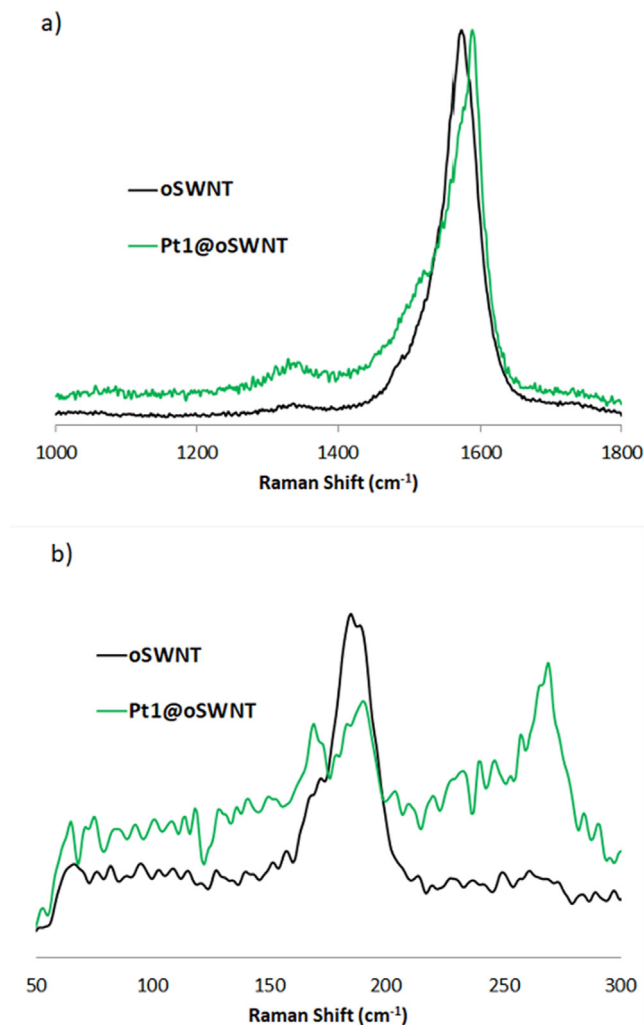


Fig. 3. a) Raman spectra of oSWNT and Pt1@oSWNT; b) Radial breathing mode (RBM) region of the Raman spectra of oSWNT and Pt1@oSWNT.

Fig. S3 at SI). However, more interesting information can be extracted from the Raman spectra (Fig. 3b). The RBM maximum of Pt1@oSWNT sample is red-shifted 5 cm⁻¹ compared to that of the pristine oSWNT sample in addition to a new band showed up at ~270 cm⁻¹. This observation is in agreement with previous reports [14,17], which showed that the encapsulation of molecules in the inner cavity of the nanotubes resulted in a local diameter expansion, especially in those tubes with larger diameter, strongly affecting the diameter-related vibrations and as red-shift in the RBM band. Consequently, such shift confirms that the encapsulation of complex 1 has proceed successfully. On the other hand, the G band of the functionalized sample red-shifts 11 cm⁻¹ compared with the position of the pristine oSWNT sample. Other authors have attributed this shift to a doping effect of the modifier towards the electronic system of the nanotube [18], which will also affect the photocatalytic properties of the material, as will be shown later.

The hybrid photocatalyst was also characterized by UV–Vis spectroscopy, showing a band at 250 nm characteristic of the π – π^* quinolate ligand transition of the Pt complex (see Figs. S4 and S5 at SI) [3]. Finally, we have quantified the Pt content of sample Pt1@oSWNT by total reflection X-ray fluorescence (TXRF) to calculate the amount of complex 1 encapsulated in the nanotubes. A 0.8% wt of Pt was determined, that corresponds with ca. 2.5% of functionalization degree.

Once Pt1@oSWNT was characterized, we explored its photocatalytic activity towards the light-driven oxidation of different organic sulfides. As a model reaction, we started the study using methyl *p*-tolyl sulfide (2a) as substrate and 1 mg of Pt1@oSWNT (Table 1, entry 1). The oxidation was carried out in 1 mL of water as solvent to test the compatibility of the catalyst in an eco-friendly medium. The reactions were performed in vials open to the air under 385 nm light irradiation. Under those reaction conditions, Pt1@oSWNT is able to fully oxidized sulfide 2a in just 6 h. Conversely, control experiments with pristine oSWNT sample or without the hybrid catalyst afforded negligible conversion (Table 1, entries 2–3). The reaction does not proceed neither in the absence of light nor inert conditions (Table 1, entries 4–5). In addition, 50% oxidation of sulfide 2a was obtained employing homogeneous complex 1 (2 mol%) as catalyst under the same experimental conditions (Table 1, entry 6). It is important to highlight that the photooxidation reaction had proceed with only 0.04 mol% of encapsulated complex 1, considering the Pt loading at the Pt1@oSWNT sample (0.8% wt).

Having this outstanding reactivity on hand, we explored the catalytic activity of Pt1@oSWNT in the scope of the photooxidation of sulfides of different nature (see Table 2). First, alkyl aryl sulfoxides 3a–3f, having different electron-donating and electron-withdrawing groups at the aromatic ring, were easily obtained in good yields after 6 h, following the reaction conditions depicted in Table 1. Noteworthy, encapsulated complex 1 successfully oxidized *p*-nitrophenyl derivative 2d, whereas we previously reported that complex 1 struggled in a homogeneous version of this test [3b]. Dialkyl sulfides, such as tetrahydrothiophene 2g or dibutylsulfide 2h could be also converted to the corresponding sulfoxides 3g and 3h in very good yields (79 % and 74 % respectively). More challenging substrates, such as phenyl benzyl sulfide 2i, a particular motif with reactive positions able to generate unwanted byproducts, was smoothly oxidized to the sulfoxide 3i with a very good performance (71%). Finally, diphenyl sulfide (2j) was found to also react, affording a 5% of the corresponding sulfoxide (3j). It is worthy to mention that all the oxidations studied were completely chemoselective, and we do not observe by ¹H NMR analysis of the crude mixture appreciable levels of either sulfone, aldehyde or any other byproduct. Moreover, the corresponding sulfoxides 3 were easily obtained after a simple filtration, without any further purification. Therefore, the catalytic performance of Pt1@oSWNT is comparable or even superior to state-of-the-art materials previously reported for this transformation (see Table S1 at SI). For instance, Pt1@oSWNT presented better catalytic parameters compared to other hybrid photocatalysts, such as a fullerene-poly siloxane, a porphyrin-amberlist, an iridium-based metalorganic framework or a thioxantone-modified silica among others. Compared to traditional catalysts, especially those based on iron systems, Pt1@oSWNT behaves with similar performance, and only more aggressive conditions (high pressure of O₂ or H₂O₂ as oxidant) could beat the performance displayed by our encapsulated hybrid photocatalyst.

Previous works described that the aromatic structure of carbon nanomaterials (nanotubes or graphene hybrid catalysts) provided synergistic catalytic effects if condensed polyaromatics are employed as substrates [14,19]. The sp² scaffold of those materials is able to interact through π – π stacking with polyaromatic substrates and preconcentrate them at the surface close to the active sites. As a result, an enhanced catalytic performance was observed. With this knowledge in hand, we studied the kinetic profile of the photooxidation of condensed aromatics sulfides naphthyl 2k and anthracyl 2l, comparing them with the model *p*-tolyl sulfide 2a (Fig. 4). All the experiments were performed using Pt1@oSWNT or homogeneous complex 1 as catalysts, air as oxygen source and

Table 1
Screening tests for the photooxidation of sulfide **2a** using **Pt1@oSWNT**.^a

Entry	Catalyst	Conversion (%) ^b
1	Pt1@oSWNT	100
2	oSWNT	NR
3	No catalyst	NR
4	No light	NR
5	No oxygen	NR
6	1 (2 mol%)	50

^a Reaction conditions: 0.1 mmol of the corresponding sulfide **2a**, 1 mg of **Pt1@oSWNT** (or 1 mg of **oSWNT** or 0.04 mol% of complex **1**) in 1 mL of H₂O was stirred at rt in open vials and irradiated under 385 nm.

^b Conversions determined by ¹H NMR of the reaction mixture. NR stands for no reaction.

Table 2
Photooxidation of different sulfides **2** using **Pt1@oSWNT** as photocatalyst.^a

^aReaction conditions: 0.1 mmol of the corresponding sulphide **2**, 1 mg of **Pt1@oSWNT** in 1 mL of H₂O was stirred at rt in open vials and irradiated under 385 nm, for 6 h.

^bYield determined by ¹H-NMR using CH₃NO₂ as internal standard.

385 nm of irradiation source. Firstly, the *p*-tolyl sulfide **2a** oxidation with **Pt1@oSWNT** required an induction period of almost 2 h, which might be ascribed to the establishment of weak interactions between **2a** and the nanotube scaffold of the catalyst in the adsorption step (Fig. 4a). After the induction period, the rate of the reaction rapidly increased, achieving full conversion in 5 h. Considering the amount of Pt encapsulated (0.8% wt, see above), **Pt1@oSWNT** is able to reach a turnover number (TON) of 2265. On the other hand, a rate-enhancement effect is observed in the oxidation of naphthyl sulfide **2k** with >95% of conversion after 2 h (TOF₀ (5 min) = 2183 h⁻¹). Indeed, no induction period is

detected even though a sigmoidal kinetic behaviour is still observed. As expected, the greater the number of aromatic rings in the sulfide, the stronger the interactions between the sulfide and the nanotube, resulting in higher reaction rates. Consequently, anthracenyl sulfide **2l** was fully oxidized in just 1 h of illumination. Indeed, the TOF₀ calculated for that sulfide is the highest calculated among the condensed aromatics, with a value of 8187 h⁻¹. To corroborate that the rate enhancement observed with **Pt1@oSWNT** is due to the nanocarbon material nature, we performed the analogous oxidation reactions using the same amount of homogeneous complex **1** (0.04 mol%, Fig. 4b). In general, lower TON were reached

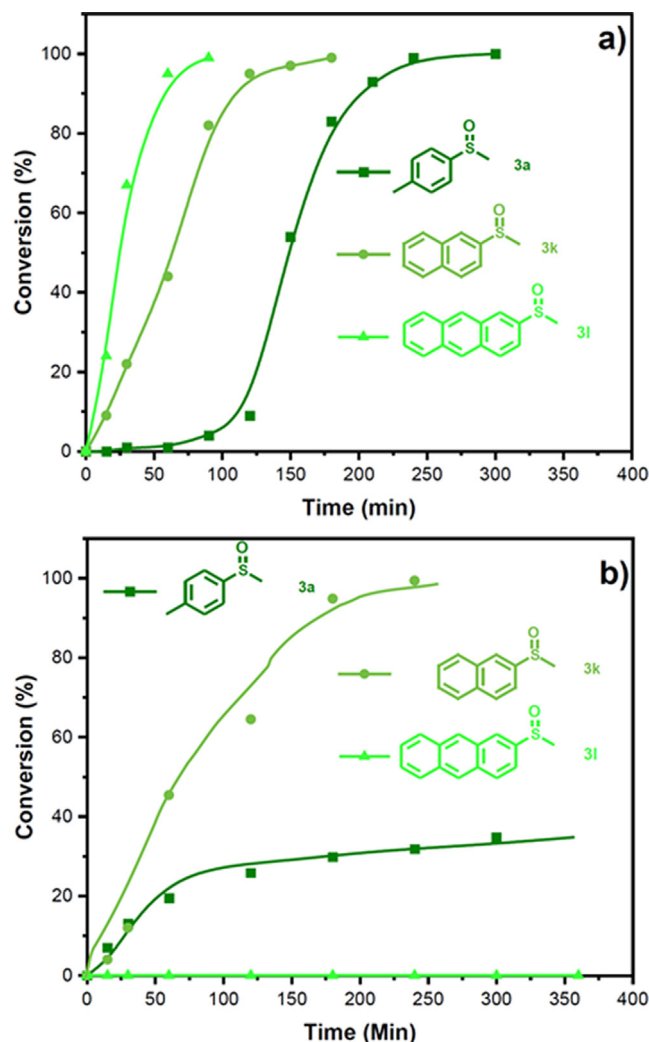


Fig. 4. Kinetic profile for the photooxidation of sulfides **2a** (*p*-tolyl), **2k** (naphthyl) and **2l** (anthracenyl) catalyzed by a) **Pt1@oSWNT** (1 mg, 0.04 mol%) and b) complex **1** (0.04 mol%) in water, under 385 nm of irradiation. Conversions determined by ^1H NMR, and lines are guides for the eyes.

under the homogeneous photocatalyst. For instance, the photooxidation of *p*-tolyl sulfide **2a** reached ~35% conversion after 5 h of reaction (TON = 786). Moreover, the catalytic performance of homogeneous complex **1** was poorer compared to **Pt1@oSWNT** when increasing the number of rings from phenyl (**2a**) to naphthyl sulfide (**2k**). Indeed, complex **1** doubled the time required to achieve the oxidation of substrate **2k** compared to the heterogeneous photocatalyst. Finally, the photooxidation of anthracenyl methyl sulfide **2l** with the homogeneous complex **1** was not possible, maybe due to parasitic homogeneous degradations prevented in the heterogeneous run. This study highlights the extra benefits of encapsulated photocatalysts into SWNT for improving the photocatalytic performance of such catalysts.

Another essential parameter to evaluate the performance of a heterogeneous catalysts is its ability to be recycled, and reused in additional reaction runs without losing its catalytic activity. To accomplish such a task, we analysed the recyclability of **Pt1@oSWNT** in the model oxidation of methyl *p*-tolyl sulfide (**2a**) in water. This performance has been compared with the endurance of the homogeneous Pt complex **1** after sequential additions of substrate **2a** under the same experimental conditions (Fig. 5a). Thus, upon full oxidation of sulfide **2a** after 6 h, the cata-

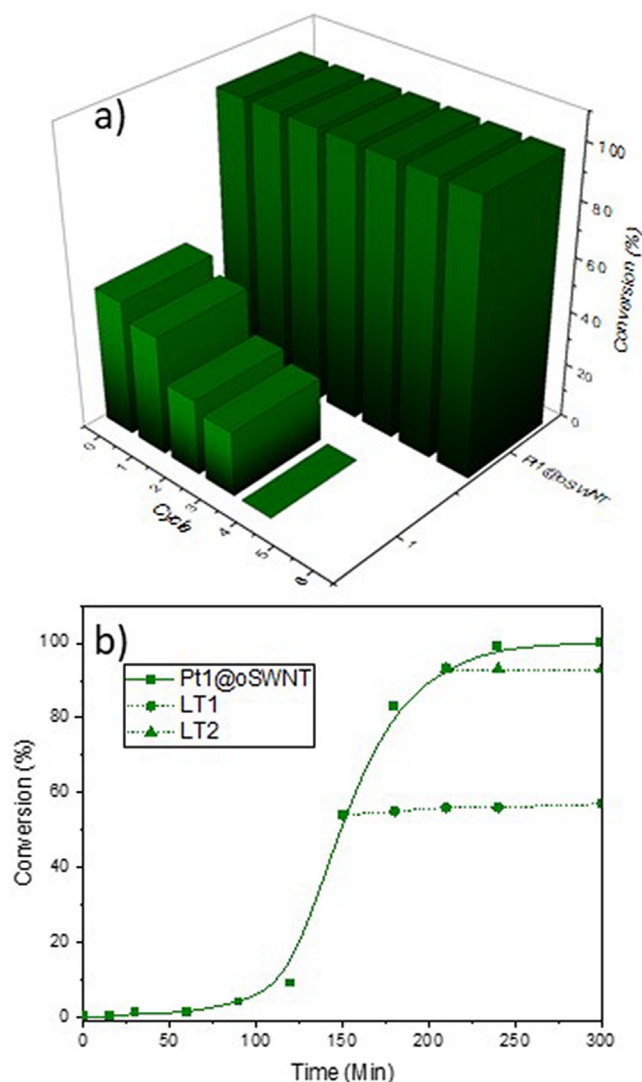


Fig. 5. a) Recyclability of heterogeneous **Pt1@oSWNT** (1 mg) and homogeneous complex **1** (0.04 mol% of Pt) in the photooxidation of **2a** (0.1 mmol) in water under 385 nm of irradiation. b) Photooxidation evolution of **2a** into **3a** using **Pt1@oSWNT** under the experimental conditions of a). LT denotes leaching test. LT1: reaction filtrated at 60% conversion. LT2: reaction filtrated at 90% conversion. Conversions determined by ^1H NMR.

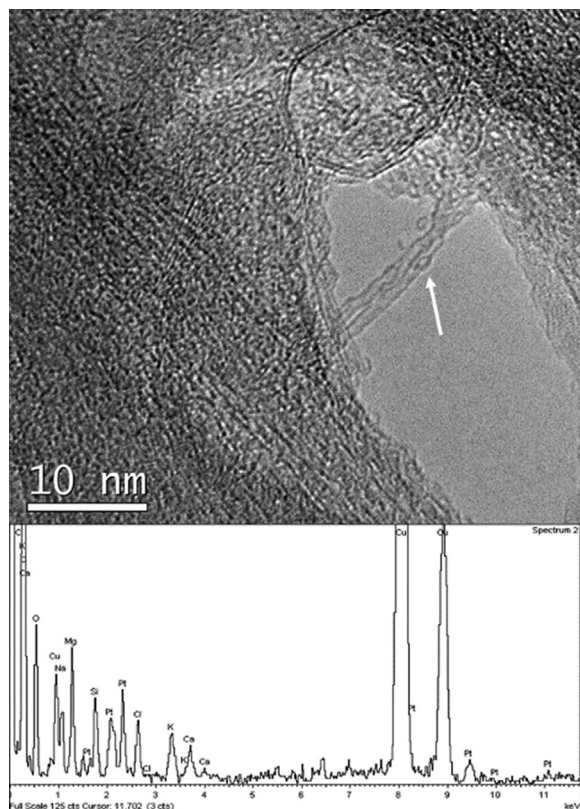
lyst, **Pt1@oSWNT**, was filtered out from the reaction, washed thoroughly with a mixture of water–acetone, dried and submitted to a new oxidation of sulfide **2a** in 1 mL of water without adding more amount of fresh catalyst. Operating in such a way, **Pt1@oSWNT** was able to maintain its catalytic activity during the 7 consecutive cycles studied. This means that 1 mg of heterogeneous photocatalyst **Pt1@oSWNT**, that contains only $4 \cdot 10^{-5}$ mmol of Pt catalyst, forms at least 108 mg of pure sulfoxide **3a** (0.7 mmol) after filtration and evaporation of the water/acetone filtrate mixture, the only waste produce in the photooxidation process. Conversely, the endurance test performed with homogeneous Pt complex **1** showed a marked decrease of its catalytic activity after the second catalytic cycle, being completely inactive after the fourth run (Fig. 5a). Moreover, to evaluate an eventual leaching processes, “hot filtration” leaching tests were performed at 60% and 90% of conversion levels (Fig. 5b). After removal of the catalyst, no further reaction was observed along the time, indicating that homogeneous catalytically active species are not present in solution.

Table 3
Quantification of the Pt content by TXRF.

Sample	Pt content
oSWNT	–
Pt1@oSWNT	0.8% wt
Pt1@oSWNT (after catalysis)	0.8% wt
Leaching test 1 ^a	0.39 ppm
Leaching test 2 ^b	0.19 ppm

^a Analysis of the reaction media after filtration at 60% conversion.^b Analysis of the reaction media after filtration at 90% conversion.

In accordance with these experiments, the analysis of the Pt content of the supernatant of the reaction after filtration by TXRF afforded very low levels of Pt (0.19–0.39 ppm, Table 3). All these results indicate that the catalytic activity observed can be only ascribed to the heterogeneous material **Pt1@oSWNT**. To confirm the stability of the complex after the reaction, the recovery sample **Pt1@oSWNT** was analysed by HRTEM, EDX and TXRF. The aspect, morphology and composition of the recovery **Pt1@oSWNT** totally matched with that of the fresh sample not submitted to the photocatalytic reactions. Indeed, complex **1** was detected clearly inside the nanotubes by HRTEM (Fig. 6), in agreement with previous experimental and theoretical results depicting that an encapsulated molecule is thermodynamically more stable inside the nanotube than outside [20]. Moreover, EDX analysis of **Pt1@oSWNT** after catalysis detected Pt content in the sample (Fig. 6), which was quantified as 0.8% wt Pt by TXRF (Table 3). In summary, the encapsulation of the Pt complex **1** into the SWNT avoids its degradation in aqueous media, and consequently, improves the robustness as well as the recyclability of the catalyst.

**Fig. 6.** TEM image and EDX spectrum of sample **Pt1@oSWNT** recovered after the catalytic study.**Table 4**Mechanistic experiments in the photooxidation of **2a** with **Pt1@oSWNT** in the presence of scavengers.

Entry	Scavenger ^a	Conversion (%) ^b
1	–	54
2	NaN ₃	23
3	1,4-dimethoxybenzene	33

^a Reaction conditions: 0.1 mmol of sulfide **2a**, 0.5 equiv of the corresponding scavenger, 1 mg of **Pt1@oSWNT** in 1 mL of H₂O was stirred at rt in open vials and irradiated under 385 nm for 2.5 h.^b Determined by ¹H NMR analysis of the reaction mixture.

Lastly, we wanted to understand the mechanism involved in the photooxidation of sulfides under **Pt1@oSWNT** catalysis. According to previous studies [21], two different pathways are possible for the photooxidation of sulfides using oxygen: a) through the formation of oxygen radical anion species via single electron transfer, or b) the formation of singlet oxygen upon an energy transfer process. Discerning between those processes is not easy, but the addition of scavengers to the reaction mixture could help to detect the key intermediates involved in the photooxidation process catalysed by **Pt1@oSWNT**. For instance, 1,4-dimethoxybenzene and sodium azide are known scavengers for electron transfer and energy transfer processes, respectively. The model reaction for the photooxidation of methyl *p*-tolyl sulfide (**2a**) using **Pt1@oSWNT** without the addition of any scavenger afforded 54% conversion into sulfoxide **3a** after 2.5 h (Table 4, entry 1). However, the photooxidation of **2a** in the presence of 0.5 equivalents of sodium azide or 1,4-dimethoxybenzene led to a decrease of the conversion values in both cases (Table 4, entries 2–3). These experiments indicated that **Pt1@oSWNT** is able to catalyze the photooxidation of sulfides by both mechanisms, single electron transfer or energy transfer reaction pathways, highlighting the catalytic versatility of the encapsulated material.

4. Conclusions

This work describes a sustainable strategy to perform the chemoselective photocatalytic oxidation of sulfides to sulfoxides. First, the hybrid photocatalyst was synthesized by endohedral functionalization of photoactive 8-oxyquinolate platinum complex **1** at the inner cavity of cap-opened Single Walled Carbon Nanotubes (sample **Pt1@oSWNT**). Secondly, the hybrid material outperforms the homogeneous counterpart in the selected photocatalytic reaction. **Pt1@oSWNT** was able to chemoselectively yield a wide variety of sulfoxides under visible light illumination in reactions carried out in water. The catalyst performed a selective oxidation preventing the formation of sulfones or any other byproduct. Furthermore, the heterogeneous catalyst at least doubled the performance of the homogeneous counterpart **1**, and also showed a strong selectivity for aromatic substrates. In addition, the heterogenization through encapsulation allowed an easy recovery of the catalyst, performing 7 consecutive reaction cycles without detecting any loss of activity or platinum leaching to the medium. Thus, the encapsulation of molecular catalysts provides a mild, selective, environmentally friendly, easy and sustainable methodology for the development of hybrid catalytic materials with increased stability and performance.

CRediT authorship contribution statement

Daniel González-Muñoz: Conceptualization, Investigation, Formal analysis. **José Alemán:** Conceptualization, Writing – review & editing, Supervision. **Matías Blanco:** Conceptualization, Investiga-

tion, Formal analysis, Writing – review & editing. **Silvia Cabrera:** Conceptualization, Writing – review & editing, Supervision.

Declaration of Competing Interest

The authors declare that they have no known competing financial interests or personal relationships that could have appeared to influence the work reported in this paper.

Acknowledgement

Financial support was provided by the Spanish Government (RTI2018-095038-B-I00), “Comunidad de Madrid”, and European Structural Funds (S2018/NMT-4367) proyectos sinérgicos I + D (Y2020/NMT-6469) and “Comunidad de Madrid” (SI1/PJI/2019-00237). M.B. thanks the Spanish Government for a Juan de la Cierva contract (IJC2019-042157-I).

Appendix A. Supplementary material

Supplementary data to this article can be found online at <https://doi.org/10.1016/j.jcat.2022.06.027>.

References

- (a) M.C. Carreño, G. Hernández-Torres, M. Ribagorda, A. Urbano, Enantiopure sulfoxides: recent applications in asymmetric synthesis, *Chem. Commun.* (2009) 6129–6144. (b) G. Sipos, E.E. Drinkel, R. Dorta, The emergence of sulfoxides as efficient ligands in transition metal catalysis, *Chem. Soc. Rev.* 44 (2015) 3834–3860. (c) M. Feng, B.H. Tang, S. Liang, X. Jiang, Sulfur containing scaffolds in drugs: synthesis and application in medicinal chemistry, *Curr. Top. Med. Chem.* 16 (2016) 1200–1216. (d) A.G. Griesbeck, S. Sillner, M. Kleczka, Catalytic Oxidation in Organic Synthesis, in: K. Muñiz (Ed.), Georg Thieme Verlag: Stuttgart, Germany, 2018 (Ch. 2).
- (a) J. Dad'ová, E. Svobodová, M. Sikorski, B. König, R. Cibulka, Photooxidation of Sulfides to Sulfoxides Mediated by Tetra-O-Acetylriboflavin and Visible Light, *ChemCatChem* 4 (2012) 620–623. (b) X. Gu, X. Li, Y. Chai, Q. Yang, P. Li, Y. Yao, A simple metal-free catalytic sulfoxidation under visible light and air, *Green Chem.* 15 (2013) 357–361. (c) C. Dang, L. Zhu, H. Guo, H. Xia, J. Zhao, B. Dick, Flavin Dibromide as an Efficient Sensitizer for Photooxidation of Sulfides, *ACS Sustainable Chem. Eng.* 6 (2018) 15254–15263. (d) R. Nasrollahi, A. Heydari-Turkmani, S. Zakavi, Kinetic and mechanistic aspects of solid state, nanostructured porphyrin diacid photosensitizers in photooxidation of sulphides, *Catal. Sci. Technol.* 9 (2019) 1260–1272. (e) Y. Gao, H. Xu, S. Zhang, Y. Zhang, C. Tanga, W. Fan, Visible-light photocatalytic aerobic oxidation of sulfides to sulfoxides with a perylene diimide photocatalyst, *Org. Biomol. Chem.* 17 (2019) 7144–7149. (f) H. Guo, H. Xia, X. Ma, K. Chen, C. Dang, J. Zhao, B. Dick, Efficient photooxidation of sulfides with amidated alloxazines as heavy-atom-free photosensitizers, *ACS Omega* 5 (2020) 10586–10595.
- (a) J.-M. Zen, S.-L. Liou, A.S. Kumar, M.-S. Hsia, An efficient and selective photocatalytic system for the oxidation of sulfides to sulfoxides, *Angew. Chem. Int. Ed.* 42 (2003) 577–579; (b) A. Casado-Sánchez, R. Gómez-Ballesteros, F. Tato, F.J. Soriano, G. Pascual-Coca, S. Cabrera, J. Alemán, Pt (II) coordination complexes as visible light photocatalysts for the oxidation of sulfides using batch and flow processes, *Chem. Commun.* 52 (2016) 9137–9140; (c) M. Vaguer, A. Ruiz-Riaguas, M. Martínez-Alonso, F.A. Jalón, B.R. Manzano, A.M. Rodríguez, G. García-Herbosa, A. Carbayo, B. García, G. Espino, Selective Photooxidation of Sulfides Catalyzed by Bis-cyclometalated Ir(III) Photosensitizers Bearing 2,2'-Dipyridylamine-Based Ligands, *Chem. Eur. J.* 24 (2018) 10662–10671; (d) A. Casado-Sánchez, M. Uygur, D. González-Muñoz, F. Aguilar-Galindo, J.L. Nova-Fernández, J. Arranz-Plaza, S. Diaz-Tendero, S. Cabrera, O. García Mancheno, J. Alemán, “8-Mercaptoquinoline as a Ligand for Enhancing the Photocatalytic Activity of Pt (II) Coordination Complexes: Reactions and Mechanistic Insights, *J. Org. Chem.* 84 (2019) 6437–6447; (e) P. Domingo-Legarda, A. Casado-Sánchez, L. Marzo, J. Alemán, S. Cabrera, Photocatalytic Water-Soluble Cationic Platinum (II) Complexes Bearing Quinolate and Phosphine Ligands, *Inorg. Chem.* 59 (2020) 13845–13857.
- (a) A. Jiménez-Almaraz, A. López-Magano, L. Marzo, S. Cabrera, R. Mas-Ballesté, J. Alemán, Imine-Based Covalent Organic Frameworks as Photocatalysts for Metal Free Oxidation Processes under Visible Light Conditions, *ChemCatChem* 11 (2019) 4916–4922; (b) S. Liu, M. Tian, S. Bu, H. Tian, X. Yang, Covalent organic frameworks toward diverse photocatalytic aerobic oxidations, *Chem. Eur. J.* 27 (2021) 7738–7744.
- (a) H. Wei, Z. Guo, X. Liang, P. Chen, H. Liu, H. Xing, “Selective Photooxidation of Amines and Sulfides Triggered by a Superoxide Radical Using a Novel Visible-Light-Responsive Metal-Organic Framework, *ACS Appl. Mater. Interfaces* 11 (2019) 3016–3023; (b) X.-N. Zou, D. Zhang, T.-X. Luan, Q. Li, L. Li, P.-Z. Li, Y. Zhao, Incorporating Photochromic Triphenylamine into a Zirconium-Organic Framework for Highly Effective Photocatalytic Aerobic Oxidation of Sulfides, *ACS Appl. Mater. Interfaces* 13 (2021) 20137–20144.
- (a) X. Liang, Z. Guo, H. Wei, X. Liu, H. Lv, H. Xing, Selective photooxidation of sulfides mediated by singlet oxygen using visible-light-responsive coordination polymers, *Chem. Commun.* 54 (2018) 13002–13005; (b) Y. Chen, J. Hu, A. Ding, Synthesis of an anthraquinone-containing polymeric photosensitizer and its application in aerobic photooxidation of thioethers, *RSC Adv.* 10 (2020) 10661–10665.
- (a) J.-P. Cao, Y.-S. Xue, N.-F. Li, J.-J. Gong, R.-K. Kang, Y. Xu, Lewis Acid Dominant Windmill-Shaped V8 Clusters: A Bifunctional Heterogeneous Catalyst for CO₂ Cycloaddition and Oxidation of Sulfides, *J. Am. Chem. Soc.* 141 (2019) 19487–19497; (b) D. Karimian, F. Zangi, Aerobic photooxidation of sulfides using unique hybrid polyoxometalate under visible light, *Catal. Commun.* 106283 (2021).
- (a) C.K.Z. Andrade, L.M. Alves, Environmentally benign solvents in organic synthesis: Current topics, *Curr. Org. Chem.* 9 (2005) 195–218. (b) R.R. Thakore, B.S. Takale in Sustainable Organic Synthesis: Tools and Strategies, in: S. Protti, A. Palmieri (Eds.), RSC, United Kingdom, 2021 (Ch. 13).
- D. González-Muñoz, A. Casado-Sánchez, I. del Hiego, S. Gómez-Ruiz, S. Cabrera, J. Alemán, Size-selective mesoporous silica-based Pt (II) complex as efficient and reusable photocatalytic material, *J. Catal.* 373 (2019) 374–383.
- A. López-Magano, A.E. Platero-Prats, S. Cabrera, R. Mas-Ballesté, J. Alemán, “Incorporation of photocatalytic Pt (II) complexes into imine-based layered covalent organic frameworks (COFs) through monomer truncation strategy, *Appl. Catal. B: Environ.* 272 (2020) 119027.
- J. Ge, Y. Zhang, S.-J. Park, Recent advances in carbonaceous photocatalysts with enhanced photocatalytic performances: A mini review, *Materials* 12 (2019) 1916.
- (a) T.B. Ogunbayo, T. Nyokong, Phototransformation of 4-nitrophenol using Pd phthalocyanines supported on single walled carbon nanotubes, *J. Mol. Catal. A: Chem.* 337 (2011) 68–76; (b) T.B. Ogunbayo, T. Nyokong, Photocatalytic transformation of chlorophenols under homogeneous and heterogeneous conditions using palladium octadecylthio phthalocyanine, *J. Mol. Catal. A: Chem.* 350 (2011) 49–55.
- (a) T. Arai, S. Nobukuni, A.S.D. Sandanayaka, O. Ito, Zinc porphyrins covalently bound to the side walls of single-walled carbon nanotubes via flexible bonds: photoinduced electron transfer in polar solvent, *J. Phys. Chem. C* 113 (2009) 14493–14499; (b) G. Lu, X. Liu, P. Zhang, L. Bao, B. Zhao, Nanoarchitectonic Composites of Mixed and Covalently Linked Multiwalled Carbon Nanotubes and Tetra-[α -(p-amino) benzyloxy] Phthalocyanine Zinc (II), *J. Nanosci. Nanotech.* 20 (2020) 2713–2721; (c) S. Rayati, A. Zamanifard, F. Nejbat, S. Hoseini, Photocatalytic potential of an immobilized free-base porphyrin for the oxidation of organic substrates, *Molecular Catalysts* 513 (2021) 111950.
- D. González-Muñoz, A. Martín-Somer, K. Strobl, S. Cabrera, P.J. de Pablo, S. Diaz-Tendero, M. Blanco, J. Alemán, Enhancing Visible-Light Photocatalysis via Endohedral Functionalization of Single-Walled Carbon Nanotubes with Organic Dyes, *ACS Appl. Mater. Interfaces* 13 (2021) 24877–24886.
- C. Martín Santos, S. Cabrera, C. Ríos-Luci, J.M. Padrón, I. López Solera, A.G. Quiroga, M.A. Medrano, C. Navarro-Ranninger, J. Alemán, Novel clioquinol and its analogous platinum complexes: importance, role of the halogen substitution and the hydroxyl group of the ligand, *Dalton Trans.* 42 (2013) 13343–13348.
- (a) V. Datsyuk, M. Kalyva, K. Papagelis, J. Parthenios, D. Tasis, A. Siokou, I. Kallitsis, C. Galiotis, Chemical oxidation of multiwalled carbon nanotubes, *Carbon* 46 (2008) 833–840; (b) M. Blanco, P. Álvarez, C. Blanco, M.V. Jiménez, J.J. Pérez-Torrente, L.A. Oro, J. Blasco, V. Cuartero, R. Menéndez, Enhancing the hydrogen transfer catalytic activity of hybrid carbon nanotube-based NHC–iridium catalysts by increasing the oxidation degree of the nanosupport, *Catal. Sci. Technol.* 6 (2016) 5504–5514.
- J.W. Jordan, G.A. Lowe, R.L. McSweeney, C.T. Stoppiello, R.W. Lodge, S.T. Skowron, J. Biskupek, G.A. Rance, U. Kaiser, D. Walsh, G.N. Newton, A.N. Khlobystov, Host–Guest Hybrid Redox Materials Self-Assembled from Polyoxometalates and Single-Walled Carbon Nanotubes, *Adv. Mater.* 31 (2019) 1904182.
- M.S. Dresselhaus, G. Dresselhaus, R. Saito, A. Jorio, Raman spectroscopy of carbon nanotubes, *Phys. Rep.* 409 (2005) 47–99.
- (a) R. Liu, C. Feng Li, Q. Chen, N.Z. Song, F. Xiao, Nitrogen-functionalized reduced graphene oxide as carbocatalysts with enhanced activity for polyaromatic hydrocarbon hydrogenation, *Catal. Sci. Technol.* 7 (2017) 1217–1226; (b) J. Calbo, A. López-Moreno, A. de Juan, J. Comer, E. Ortí, E.M. Pérez, Understanding noncovalent interactions of small molecules with carbon nanotubes, *Chem. Eur. J.* 23 (2017) 12909–12916; (c) M. Blanco, B. Nieto-Ortega, A. de Juan, M. Vera-Hidalgo, A. López-Moreno, S. Casado, L.R. González, H. Sawada, J.M. González-Calbet, E.M. Pérez, Positive

and negative regulation of carbon nanotube catalysts through encapsulation within macrocycles, *Nat. Commun.* 9 (2018) 2671;
 (d) D. Mosconi, M. Blanco, T. Gatti, L. Calvillo, M. Otyepka, A. Bakandritsos, E. Menna, S. Agnoli, G. Granozzi, Arene CH insertion catalyzed by ferrocene covalently heterogenized on graphene acid, *Carbon* 143 (2019) 318–328;
 (e) M. Blanco, S. Cembellín, S. Agnoli, J. Alemán, Ruthenium-p-cymene

Complex Side-Wall Covalently Bonded to Carbon Nanotubes as Efficient Hybrid Transfer Hydrogenation Catalyst, *ChemCatChem* 13 (2021) 5156–5165.
 [20] D.A. Britz, A.N. Khlobystov, Noncovalent interactions of molecules with single walled carbon nanotubes, *Chem. Soc. Rev.* 35 (2006) 637–659.
 [21] S.M. Bonesi, I. Manet, M. Freccero, M. Fagnoni, A. Albini, Photosensitized oxidation of sulfides, *Chem. Eur. J.* 12 (2006) 4844–4857.